

Role of core-scattered closed orbits in nonhydrogenic atoms

P. A. Dando,¹ T. S. Monteiro,¹ D. Delande,² and K. T. Taylor³

¹*Department of Physics and Astronomy, University College London, Gower Street, London, WC1E 6BT, United Kingdom*

²*Laboratoire Kastler-Brossel, 4 place Jussieu, Tour 12, F-75252 Paris Cedex 05, France*

³*Department of Applied Mathematics and Theoretical Physics, Queen's University Belfast, Belfast, BT7 1NN, United Kingdom*

(Received 8 November 1995)

While both diamagnetic and Stark spectra of hydrogen can be analyzed accurately in terms of classical orbits, in nonhydrogenic atoms the multielectron core induces additional spectral modulations that cannot be analyzed reliably in terms of standard periodic orbit-type theories. However, by extending closed-orbit theory to include core-scattered waves consistently, both diamagnetic and Stark photoabsorption spectra of nonhydrogenic Rydberg atoms at constant scaled energy can be analyzed semiclassically using only the closed orbits of the corresponding hydrogenic systems. Frequencies and amplitudes of the core-scattered modulations, as well as corrected amplitudes for contributions from repetitions of primitive hydrogenic orbits, are found to be in excellent agreement with quantum results. We consider whether these nonhydrogenic systems correspond to quantum chaos. [S1050-2947(96)02807-7]

PACS number(s): 03.65.Sq, 05.45.+b, 32.60.+i

I. INTRODUCTION

Our understanding of quantum systems associated with chaotic motion in the classical limit—a study popularly termed “quantum chaos”—remains incomplete. In particular, the quantization of such systems, that is the determination of the eigenvalues and eigenstates of the quantum system in terms of classical quantities, continues to provide one of the fundamental challenges to physics. The most successful approaches to the quantization of nonintegrable, time-independent Hamiltonian systems have been based on the Gutzwiller trace formula [1], which, within a semiclassical framework, expresses the density of states of the quantum system as an infinite sum of contributions from all periodic orbits of the underlying classical system. The analysis relies on the derivation of a semiclassical Green's function, which is supposedly valid for strongly chaotic systems in the limit $\hbar \rightarrow 0$. In this paper we show—in the specific case of nonhydrogenic Rydberg atoms in static external fields—how the presence of an ionic core leads to pure quantum effects that cannot be described by standard periodic orbit-type theories and how these effects can be incorporated successfully in the theory.

Highly excited (Rydberg) atoms in strong external fields have furnished some of the most rewarding case studies of real quantum systems that are observable in the laboratory and for which the corresponding classical motion exhibits chaos [2]. Of such systems, the diamagnetic hydrogen atom is the most readily accessible for theoretical study. A special feature of this system is its scaling property: the classical motion does not depend on the electron energy and the magnetic field strength separately but only on a single parameter, the *scaled* energy. As this parameter is varied the classical motion undergoes a gradual transition from regularity to full chaos. With the development of scaled variable spectroscopy [3], together with methods for calculating fully quantal spectra at constant scaled energy, it has been possible to make direct comparisons between the quantum and classical dynamics of the diamagnetic hydrogen atom [4,5]. In particu-

lar, the frequencies and amplitudes of the long-range modulations in the density of states have been successfully predicted using periodic orbit theory [6]. Similar modulations in the observed photoabsorption spectrum have also been reproduced and interpreted semiclassically using a theory developed by Du and Delos [7] (see also Bogomolny [8] and Alber [9]). Analogous to Gutzwiller's periodic orbit formula, the closed-orbit formula [7] represents the energy-averaged photoabsorption spectrum in the classically chaotic regime as a sum of contributions from isolated closed classical orbits, which start from, and return to, the nucleus.

The theoretical description of nonhydrogenic atoms in external fields is less well developed. Indeed, one of the few studies to consider the connections between quantum and classical dynamics of such systems interpreted features of the quantum spectrum in terms of a semiclassical analysis of hydrogen [10]. Recently, a growing body of theoretical and experimental evidence on spectra and wave-packet dynamics of nonhydrogenic atoms in external fields [11–15] has suggested that the ionic core induces important dynamical effects not seen in hydrogen.

Most theoretical quantum solutions of the diamagnetic nonhydrogenic problem [11,12,16–18] follow a suggestion of Clark and Taylor [19] who noted that the problem splits into two regions: an outer region, where the core is negligible and the Hamiltonian is hydrogenic, and an inner region where the field is negligible. In the latter case, the interaction of the outer electron with the ionic core can be accounted for by a set of phase shifts dependent on angular momentum l —the quantum defects, μ_l (see, for example, Seaton [20]). Separate solutions are obtained in the two regions and matched at a boundary using an R -matrix approach.

While the hydrogenic scaling property does not hold in the core region of nonhydrogenic atoms, it is appropriate to apply the same scaling transformation to nonhydrogenic atoms because the core region is very small compared with the size of the highly excited Rydberg states. The first fully quantum mechanical calculation on nonhydrogenic atoms in a magnetic field at fixed scaled energies, permitting direct

comparison between quantum and classical dynamics [11], showed strong resonance structures in the Fourier transformed spectra, which seemingly could not be explained by hydrogenic orbits, together with a reduction in the modulations of the long-period orbits. These observations have since been confirmed by experimental measurements of diamagnetic helium atoms and the additional modulations identified as being due to combinations of periodic hydrogenic orbits that arise from scattering with the core [12]; similar structures have been found in the experimental Stark spectra of lithium [14,15] and the experimental spectra of rubidium in crossed electric and magnetic fields [13]. Further theoretical calculations showed the nearest-neighbor spacing statistics to be displaced towards the “chaotic” (Wigner) limit, even for low scaled energies where the hydrogenic problem is almost regular [11,21]. Recent calculations have shown that the Stark spectrum of lithium exhibits similar behavior [15] and has led to the claim that nonhydrogenic systems provide further examples of quantum chaos.

However, studies of quantum phase space distributions (Wigner functions) have suggested that this is not the full story [21]. While the Wigner distributions of diamagnetic nonhydrogenic atoms do explore a larger fraction of phase space than their hydrogenic counterparts, they do not have the more “ergodic” appearance of those for the hydrogen atom in the classically chaotic regime. Indeed, the nonhydrogenic phase space distributions show toruslike structures but with each eigenstate now linked to several “tori” rather than just one as in the hydrogenic case; clearly this is not the signature of a true chaotic system.

In an attempt to shed some light on this apparent paradox, Dando *et al.* [22] carried out a classical calculation for diamagnetic nonhydrogenic atoms, employing a short-range “model” potential to describe the non-Coulombic nature of the ionic core. At scaled energies where the hydrogenic problem is very nearly regular, it was shown that trajectories of the nonhydrogenic system, although typically ergodic, remain on a torus of hydrogen once outside the core region. Hence trajectories are able to see most of phase space by a process of “torus-hopping”: regular motion interspersed with scattering by the core. The periodic orbits were found to have large Liapunov exponents and the dynamics is extremely unstable. However, a recent variation of this method [27], which involves superposing contributions from thousands of such unstable periodic orbits, was applied successfully to atomic photoabsorption spectra. In that case, stability parameters were calculated with the core potential “switched off” at the start and final return of the trajectory to the core region. Hence the stability parameters for first traversals of the primitive hydrogenic orbits remain unchanged. However, the method is computationally extremely intensive since it involves the calculation of thousands of classical orbits for each different atom in a regime where the standard semiclassical model for hydrogen requires only a couple of dozen. Further, it gives qualitative agreement or less in many circumstances—for example, it becomes increasingly less capable of reproducing the quantum results for smaller atoms such as helium. But it is important in helping to demarcate the boundary between an approximate semiclassical regime and the regime of “diffractive” scattering (i.e., the regime where the de Broglie wavelength of the electron is compa-

rable to or larger than the core and hence wave effects must be considered).

The only adequate approach, valid for any regime of atomic core scattering in Rydberg atoms, must allow for the breakdown of classical path methods at the core. Such a method was first proposed by Gao and Delos [24] in their pioneering work on a semiclassical description of nonhydrogenic atoms in external fields, which incorporated the quantum defects describing the ionic core in the closed-orbit sum of *hydrogenic* orbits. They described the effects of spin-orbit coupling in the initial state, the effects of nonhydrogenic radial dipole integrals, and the effects of quantum defects associated with the ionic core; these quantities all affect the angular distribution of the outgoing waves. However, the effect of the nonhydrogenic core-scattered waves was found to be insignificant and neglected from the final calculation so that the core effects only resulted in slight shifts of the resonance positions in the absorption spectra [25].

It is now amply clear that, in general, the core-scattered waves must be included in any semiclassical approach. The ionic core scatters waves from one closed orbit to another. The Fourier transform of the absorption spectrum (the “recurrence spectrum”) should show two effects. (i) There should be core-scattered contributions (“combination recurrences”) due to the electron traveling along one closed orbit and then being scattered by the ionic core on to another closed orbit. (ii) The core should cast a “shadow” in the backwards direction thus reducing the recurrence strength on subsequent returns to the nucleus of each orbit. The closed-orbit formula given in Ref. [24] does not include this effect and so leads to a spectrum which is qualitatively different from that which is observed.

By starting with the physical picture of the photoabsorption process suggested by Gao and Delos [24], but including the core-scattered waves consistently, we have recently been able to extend closed-orbit theory to successfully reproduce the core-induced phenomena [26]. The advantage of our semiclassical approach is that it allows us to describe the dynamics of relatively complicated multielectron systems in terms of the simpler, yet closely related, hydrogenic system.

In this paper we present a detailed account of our semiclassical method. We provide further comparisons with fully quantal calculations for nonhydrogenic atoms in external fields generated using a recently developed method, which enables the calculation of the quantum constant scaled energy spectrum of nonhydrogenic atoms for very high-lying states, closer to the semiclassical limit [12]. In addition to the diamagnetic nonhydrogenic spectra considered previously [26], we also apply our theory to the Stark spectrum of lithium. The corresponding hydrogenic problem is integrable and hence the classical motion does not display the exponential proliferation of closed orbits characteristic of the diamagnetic problem. This allows us to evaluate the closed-orbit sum to a considerably higher resolution than is numerically convenient in the diamagnetic case. The excellent agreement obtained with spectra obtained from quantum calculations provides further justification of our method.

The remainder of this paper is organized as follows: in Sec. II we give a brief review of closed-orbit theory as presented by Delos and co-workers [7,24]. In Sec. III we show how this theory can be extended to include the core-scattered

contributions consistently. Section IV gives both the diamagnetic and Stark Hamiltonians for the hydrogen atom and shows how these Hamiltonians can be scaled to remove the separate dependence on electron energy and field strength. In Sec. V we outline the iterative procedure that we use to calculate the photoabsorption spectrum semiclassically. The results of our calculations are presented in Sec. VI where we compare the semiclassical photoabsorption spectra of both diamagnetic and Stark nonhydrogenic atoms, calculated using our semiclassical approach, with fully quantum mechanical spectra. Finally, in Sec. VII we present some discussion and our conclusions.

II. REVIEW OF CLOSED-ORBIT THEORY

Our semiclassical approach extends the work of Delos and co-workers [7,24] in which the energy-averaged photoabsorption spectra of atoms in external fields is expressed as a sum of contributions from closed orbits of the corresponding classical system. The theory underlying the so-called closed-orbit formula has been presented previously in great detail [7,24] so we give only a brief outline of the salient features.

When an atom absorbs a photon, the electron propagates outwards in a near zero-energy Coulomb wave. At sufficiently large distances from the nucleus the wave propagates semiclassically along classical trajectories with the wave fronts perpendicular to those trajectories. Eventually, the trajectories and their associated waves are turned back by the action of the external field. Some of the trajectories return to the vicinity of the nucleus and the waves associated with them, which are (cylindrically modified) incoming Coulomb

waves, interfere with the outgoing waves generating oscillations in the absorption spectrum. The incoming waves produce, in turn, Coulomb scattered waves and, for nonhydrogenic atoms, core-scattered waves. The Coulomb scattered waves are strongly backwardly focused and back trace the orbit resulting in repeated traversals of the trajectory. In this respect, quantal and classical Coulomb scattering are equivalent. The core-scattered waves, on the other hand, redistribute amplitude into other closed orbits, isotropically for an s -wave ($l=0$) quantum defect or as $\cos\theta$ for p -wave scattering. Gao and Delos [24] concluded that the contribution of the core-scattered waves to the averaged absorption cross-section was negligibly small [25].

The result is a formula for the average oscillator-strength density that can be written as a combination of a smooth background term plus a set of sinusoidal oscillations of the form

$$f(E) = \sum_n \sum_k C_k^n(E) \sin[\Delta_k^n(E)], \quad (1)$$

which arise from the interference of semiclassical waves associated with closed orbits of an electron of energy E . Each different orbit is indexed by k and the repetitions of each orbit are labeled by n . The ‘‘recurrence amplitude,’’ $C_k^n(E)$, for the n th repetition of the k th closed orbit, contains information about the stability of the orbit, via the semiclassical amplitude, A_k^n , its initial and final angles, θ_i^k and $\theta_f^{k,n}$, and the matrix element of the dipole operator between the initial state and a zero-energy Coulomb wave: in atomic units this is given by the formulas,

$$C_k^n(E) = \begin{cases} (E - E_i) 2^{19/4} \pi^{3/2} (\sin\theta_i^k \sin\theta_f^{k,n})^{1/2} r_0^{-1/4} \mathcal{Y}(\theta_i^k) \mathcal{Y}^*(\theta_f^{k,n}) A_k^n & (k \neq 0) \\ (E - E_i) 2^{9/2} \pi r_0^{-1/2} \mathcal{Y}(\theta_i=0) \mathcal{Y}^*(\theta_f=0) A_0^n & (k=0). \end{cases} \quad (2)$$

The ‘‘recurrence phase,’’ $\Delta_k^n(E)$, depends on the action of the closed orbit, $S_k^n = n \oint_k \mathbf{p} \cdot d\mathbf{q}$, together with an additional phase that is computed from the Maslov Index, α_k^n , and other geometrical considerations,

$$\Delta_k^n(E) = \begin{cases} S_k^n - \frac{\pi}{2} \alpha_k^n - \frac{3\pi}{4} & (k \neq 0) \\ S_0^n - \frac{\pi}{2} \alpha_0^n - \frac{\pi}{2} & (k=0). \end{cases} \quad (3)$$

A detailed derivation of Eqs. (2) and (3) for C_k^n and Δ_k^n , respectively, is given in Refs. [7] and [24].

III. CORE SCATTERING AND CLOSED-ORBIT THEORY

It is now apparent that, in general, the core induces important dynamical effects [11–15,21,26] and, therefore, it is necessary to include the contribution of the core-scattered waves in any semiclassical approach. A physical picture of

the core-scattering process was first presented by Gao and Delos [24] and outlined in Sec. II. We proceed by showing how the core-scattered waves can be included within the closed-orbit formalism.

In order to solve this problem we begin by noting that there are three characteristic spatial regions as far as the dynamics of the excited electron is concerned; the *core region*, the surrounding *Coulomb region*, where the dynamics of the excited electron is predominantly determined by the Coulomb force of the ionic core, and the *outer region* where the influence of the external field is at least as important as the Coulomb force of the ionic core. Our approach is to solve the problem quantum mechanically in the core and Coulomb regions, semiclassically in the Coulomb and outer regions, and then to match these two solutions in the Coulomb region where both are valid.

A. Solution in the core and Coulomb regions

In both core and Coulomb regions we can neglect the external field. The core region extends only a few Bohr radii

around the atomic nucleus and contains the effect of the laser excitation of the energetically low-lying initial-state wave function. Outside the core region is the surrounding Coulomb region, which extends to a few hundred Bohr radii from the nucleus. There we may use quantum defect theory [20] to obtain an expression for the wave function that is valid throughout the Coulomb region (but not the core). The general solution at $\mathbf{r}=(r, \vartheta, \varphi)$ can be written as

$$\Psi(\mathbf{r}) = \Phi_0(\mathbf{r}) + \sum_j \mathcal{N}_j [\psi_j^{(+)}(\mathbf{r}) + \psi_j^{(-)}(\mathbf{r})], \quad (4)$$

and consists of a linear superposition of incoming, $\psi_j^{(-)}$, and outgoing waves, $\psi_j^{(+)}$, which arise from the scattering of an electron that approaches the nucleus, from a source at infinity, at an angle θ_j to the z axis. Following Delos and co-workers [7,24], we consider only highly excited states whose energy is very close to the ionization threshold. Then, the incoming and outgoing waves are cylindrically modified, zero-energy Coulomb waves with the phase shifts (quantum defects) that describe the core. The initial outgoing wave, Φ_0 , describes the interaction of the laser with the well-localized, energetically low-lying, initial state.

B. Solution in the Coulomb and outer regions

In the outer region, which typically lies beyond 30 Bohr radii from the nucleus, we can use semiclassical methods [28] to write the wave function as a sum of contributions from classical trajectories provided we know the wave function on an initial surface. For the systems considered here, the Hamiltonian has cylindrical symmetry and hence the three-dimensional wave function can be written as

$$\begin{aligned} \Psi_{\text{sc}}(\mathbf{r}) = & \sum_j \Psi_0^{(+)}(r_0, \theta_j^i) A_j(r, \vartheta) \\ & \times \exp \left[i \left(S_j(r, \vartheta) - \alpha_j \frac{\pi}{2} \right) \right] e^{im\varphi}, \end{aligned} \quad (5)$$

where $\Psi_0^{(+)}$ is an outgoing wave function known on the initial surface at $r=r_0$ and atomic units have been used. The sum is taken over all trajectories, j , which reach $\mathbf{r}=(r, \vartheta, \varphi)$ having left the surface r_0 at angles θ_j^i to the z axis. Core effects are negligible in this region and so these trajectories are hydrogenic. The amplitude of the semiclassical wave, A_j , contains information about the stability of the trajectory, j , and, for $\theta_j^i \neq 0, \pi$, is given by

$$A_j(r, \vartheta) = \left| \frac{J_2(0, \theta_j^i)}{J_2(t, \theta_j^i)} \right|^{1/2} \left| \frac{r_0^2 \sin \theta_j^i}{r^2 \sin \vartheta} \right|^{1/2}, \quad (6)$$

where the two-dimensional Jacobian,

$$J_2(t, \theta_j^i) = \frac{\partial(r, \theta)}{\partial(t, \theta_j^i)}, \quad (7)$$

can be calculated from the motion of neighboring trajectories.

The phase of the semiclassical wave consists of two terms: the classical action $S_j = \int \mathbf{p}_j \cdot d\mathbf{q}_j$ accumulated along

the trajectory j , and the Maslov index, α_j , which is an integer equal to the number of caustics and foci [where $J_2(t, \theta_j^i) = 0$] encountered by the trajectory.

Cylindrical symmetry means that the z component of angular momentum, and hence the magnetic quantum number m , is conserved and so the azimuthal angle φ is an ignorable coordinate; henceforth we neglect the dependence of the wave functions on this angle.

C. Matching of solutions

In order to determine the unknown coefficients \mathcal{N}_j of Eq. (4) we match the asymptotic forms of the incoming and outgoing components of the wave function obtained for the core and Coulombic regions, Eq. (4), to those of the semiclassical wave function, Eq. (5). We carry out this matching procedure on the sphere of radius r_0 , which we assume to lie within the Coulomb zone where both Eq. (4) and Eq. (5) are valid. For laboratory strength fields, any distance between 30 to 100 Bohr radii is acceptable; Delos and co-workers [7,24] suggest $r_0 = 50$ Bohr radii. The crucial point is that the matching should take place at a radius sufficiently large for the semiclassical approximation, Eq. (5), to be valid but small enough for the effect of the external field to be neglected so that the quantum defect solution, Eq. (4), still holds. Of course, the final result for the photoabsorption cross section will be independent of the matching radius r_0 .

By matching the outgoing components of each of the wave functions Eqs. (4) and (5) at the starting angles $\vartheta = \theta_j^i$ of each trajectory that returns to the surface at r_0 we obtain an expression for the outgoing wave function, $\Psi_0^{(+)}$, on the surface r_0 ,

$$\Psi_0^{(+)}(r_0, \theta_j^i) = \Phi_0(r_0, \theta_j^i) + \sum_k \mathcal{N}_k \psi_k^{(+)}(r_0, \theta_j^i). \quad (8)$$

Matching the incoming waves at the final angles $\vartheta = \theta_j^f$ of the returning trajectories gives

$$\Psi_{\text{sc}}(r_0, \theta_j^f) = \mathcal{N}_j \psi_j^{(-)}(r_0, \theta_j^f). \quad (9)$$

On using the expressions for $\Psi_0^{(+)}$, Eq. (8), and Ψ_{sc} , Eq. (5), we obtain the following equation for the \mathcal{N}_j 's:

$$\begin{aligned} & \left\{ \Phi_0(r_0, \theta_j^i) + \sum_k \mathcal{N}_k \psi_k^{(+)}(r_0, \theta_j^i) \right\} A_j(r_0, \theta_j^f) \\ & \times \exp \{ i(S_j - \alpha_j \pi/2) \} = \mathcal{N}_j \psi_j^{(-)}(r_0, \theta_j^f). \end{aligned} \quad (10)$$

The result is a set of coupled linear equations for the \mathcal{N}_j 's; potentially, each orbit is coupled to every other by the scattering process. In order to solve Eq. (10) for the \mathcal{N}_j 's we use the closed forms and partial wave expansions for Φ_0 , $\psi_j^{(+)}$, and $\psi_j^{(-)}$ as given by Delos and co-workers [7,24].

D. Outgoing Coulomb waves

The required asymptotic form for Φ_0 is obtained by considering the action of an outgoing zero-energy, Green's function on the dipole operator and initial state [7,24],

$$\Phi_0(r_0, \theta_i^j) = -i\pi^{1/2} 2^{3/4} r_0^{-3/4} e^{i(\sqrt{8r_0} - 3\pi/4)} \mathcal{Y}(\theta_i^j), \quad (11)$$

where the angular functions

$$\mathcal{Y}(\theta) = \sum_{l=|m|}^{\infty} (-1)^l e^{i\pi\mu_l} B_{lm} Y_{lm}(\theta, 0) \quad (12)$$

depend on the action of the dipole operator, \hat{D} , on the initial-state wave function, ϕ_i , and on the quantum defects, μ_l , of the ionic core. The coefficients, B_{lm} , are determined by the photoabsorption process:

$$B_{lm} = \sqrt{8} \int \hat{D}(\mathbf{r}') \phi_i(\mathbf{r}') R_l^{0,\text{reg}}(r') Y_{lm}^*(\vartheta', \varphi') d\mathbf{r}', \quad (13)$$

where $R_l^{0,\text{reg}}(r)$ is a regular zero-energy radial wave function, which, outside the ionic core, can be written as a linear combination of Bessel functions with prefactors that depend on the quantum defects, μ_l ,

$$R_l^{0,\text{reg}} = \cos\pi\mu_l \frac{J_{2l+1}(\sqrt{8r})}{\sqrt{8r}} - \sin\pi\mu_l \frac{Y_{2l+1}(\sqrt{8r})}{\sqrt{8r}}. \quad (14)$$

For the hydrogenic case, the B_{lm} 's can be evaluated analytically. However, for nonhydrogenic atoms, we know neither the exact form of the initial wave function nor the regular zero-energy radial wave function inside the core region and so the B_{lm} 's are unknown. They are, however, constant and, for the dipole transitions considered in Sec. VI below (π transitions from an s state), only one B_{lm} coefficient (namely, B_{10}) is nonzero, leading only to a constant multiplicative factor in the final spectra.

E. Incoming waves

The incoming waves, $\psi_j^{(-)}$, are cylindrically modified, zero-energy Coulomb waves and, for $r=r_0$ are given by [7]

$$\psi_j^{(-)}(r_0, \theta_f^j) = (-1)^m \frac{\exp\{-i(\sqrt{8r_0} - \pi/2)\}}{\pi\sqrt{8r_0}\sin\theta_f^j} \quad (\theta_f^j \neq 0, \pi). \quad (15)$$

For $m=0$ it is also possible for incoming waves to approach the nucleus along the field axis, that is the waves are associated with closed orbits for which $\theta_f^j=0$ or $\theta_f^j=\pi$. In this case, the closed-form expression for the incoming waves, $\psi_j^{(-)}$, is [24]

$$\psi_j^{(-)}(r_0, \theta_f^j) = \frac{1}{2} \left(\frac{2}{\pi\sqrt{8r_0}} \right)^{1/2} \exp\{-i(\sqrt{8r_0} - \pi/4)\} \quad (\theta_f^j = 0, \pi). \quad (16)$$

F. Outgoing scattered waves

As noted by Gao and Delos [24] the scattered wave function, $\psi_j^{(+)}$, is composed of two parts,

$$\psi_j^{(+)}(\mathbf{r}) = \psi_{\text{Coul}}^j(\mathbf{r}) + \psi_{\text{core}}^j(\mathbf{r}). \quad (17)$$

The core-scattered waves, ψ_{core}^k , describe the redistribution of amplitude from a trajectory approaching the nucleus along trajectory, k , into trajectory, j , by the compact ionic core and have the partial wave expansion [24]

$$\psi_{\text{core}}^k(r_0, \theta_i^j) = \left(\frac{2\pi^2}{r_0^3} \right)^{1/4} \sum_{l=|m|}^{\infty} (-1)^{l-m} Y_{lm}^*(\theta_f^k, 0) Y_{lm}(\theta_i^j, 0) e^{i(\sqrt{8r_0} - l\pi - 3\pi/4)} (e^{2i\pi\mu_l} - 1). \quad (18)$$

The Coulomb scattered wave, ψ_{Coul}^j , is strongly back-focused and, on the surface at r_0 , is simply related to the incoming wave, $\psi_j^{(-)}(r_0, \theta_f^j)$ of Eq. (15), by

$$\psi_{\text{Coul}}^j(r_0, \theta_f^j) = \psi_j^{(-)}(r_0, \theta_f^j) e^{i(2\sqrt{8r_0} - \pi)} \quad (\theta_f^j \neq 0, \pi), \quad (19)$$

with a similar expression holding for $\theta_f^j=0, \pi$. Thus the Coulomb scattered wave results in the semiclassical wave retracing its path along the closed orbit, with a phase change of $(2\sqrt{8r_0} - \pi)$, thus giving rise to repetitions of the orbit. The first term of the phase difference corresponds to the

increase in the classical action of the orbit from the surface at r_0 to the nucleus and back to r_0 ; the second term is naturally incorporated into the Maslov index and shows that this increases by 2 at each return of the closed orbit to the nucleus. Taking this into account, we see that the dependence of the \mathcal{N}_j 's on ψ_{Coul}^j can be eliminated from Eq. (10) simply by including all repetitions of the closed orbits.

G. Oscillator strength

On allowing for the effect of ψ_{Coul}^j and substituting Eqs. (11), (15), and (18) into Eq. (10) we arrive at our final equation for the \mathcal{N}_j 's:

$$\mathcal{N}_j = \left\{ \mathcal{D}_j(\theta_j^i) + \sum_{k,p} \mathcal{N}_k \mathcal{B}_j^{k,p}(\theta_j^i) \right\} \sum_n \mathcal{A}_j^n \exp\{i(S_j^n - \alpha_j^n \pi/2 - \phi_j)\}, \quad (20)$$

where $\phi_j = \pi/2$ for $\theta_j^i = 0$ or $\theta_j^i = \pi$ and $\phi_j = 3\pi/4$ otherwise. For convenience, we have written the core-scattered contributions in the form

$$\mathcal{B}_j^{k,p}(\theta_j^i) = \begin{cases} i2^{7/4} \pi^{3/2} \sum_{l=|m|}^{\infty} Y_{lm}^*(\theta_f^{k,p}, 0) Y_{lm}(\theta_i^j, 0) (e^{2\pi i \mu_l} - 1) & (\theta_i^j \neq 0, \pi) \\ 2^{3/2} \pi \sum_l Y_{l0}^*(\theta_f^{k,p}, 0) Y_{l0}(\theta_i^j, 0) (e^{2\pi i \mu_l} - 1) & (\theta_i^j = 0, \pi), \end{cases} \quad (21)$$

while the initial outgoing contributions have been expressed as

$$\mathcal{D}_j = \begin{cases} 2^{9/4} \pi^{3/2} \mathcal{Y}(\theta_j^i) & (\theta_j^i \neq 0, \pi) \\ -i4\pi \mathcal{Y}(\theta_j^i) & (\theta_j^i = 0, \pi), \end{cases} \quad (22)$$

with $\mathcal{Y}(\theta)$ given by Eq. (12) above. The semiclassical amplitude is now written as

$$\mathcal{A}_j^n = \begin{cases} r_0^{-1/4} \sin \theta_f^{j,n} A_j^n & (\theta_j^i \neq 0, \pi) \\ r_0^{-1/2} A_j^n & (\theta_j^i = 0, \pi), \end{cases} \quad (23)$$

where A_j^n , S_j^n , α_j^n , and $\theta_f^{j,n}$ are the amplitude, action, Maslov index, and final return angle, respectively, for the n th return to the nucleus of the j th closed orbit and can be calculated from the properties of the orbit on its first return [29]. The contribution from the core-scattered waves also includes a sum over all repetitions, p . It should be emphasized that all the quantities in Eq. (20) no longer depend on the matching radius r_0 and can be evaluated using the hydrogenic closed orbits starting and ending at the nucleus (not at $r=r_0$).

In order to solve Eq. (20) for the \mathcal{N}_j 's, we find it convenient to use an iterative procedure, which is outlined in Sec. V below. Once the \mathcal{N}_j 's have been found we can then obtain the required absorption rate, the oscillatory part of which is simply

$$f(E) = -\frac{2(E-E_i)}{\pi} \text{Im} \sum_j \mathcal{N}_j \int \hat{D}^*(\mathbf{r}) \phi_i^*(\mathbf{r}) [\psi_j^{(+)}(\mathbf{r}) + \psi_j^{(-)}(\mathbf{r})] d\mathbf{r}, \quad (24)$$

where E_i is the energy of the initial state ϕ_i . The integral can be readily evaluated by expressing the wave functions in terms of zero-energy Coulomb functions. For nonhydrogenic atoms this is given by Eq. (7.7) of Ref. [24],

$$\begin{aligned} & (-1)^m \int \hat{D}^*(\mathbf{r}) \phi_i^*(\mathbf{r}) [\psi_j^{(+)}(\mathbf{r}) + \psi_j^{(-)}(\mathbf{r})] d\mathbf{r} \\ & = 2\sqrt{2}\pi \mathcal{Y}^*(\theta_j^i), \end{aligned} \quad (25)$$

where $\mathcal{Y}^*(\theta)$ is the ‘‘unexpected conjugate’’ [24] of $\mathcal{Y}(\theta)$, Eq. (12),

$$\mathcal{Y}^*(\theta) = \sum_l (-1)^l e^{i\pi \mu_l} B_{lm}^* Y_{lm}^*(\theta, 0). \quad (26)$$

Hence, the oscillatory part of the density of oscillator strengths has the final simple expression

$$f(E) = -\frac{2(E-E_i)}{\pi} \text{Im} \sum_j \mathcal{N}_j (-1)^m \sqrt{8}\pi \mathcal{Y}^*(\theta_j^i). \quad (27)$$

It is this expression, together with the \mathcal{N}_j coefficients obtained by solving Eq. (20), that is used in Sec. VI to compute the Fourier transforms of the density of oscillator strengths shown in the figures. For the photoabsorption from s states using π polarization, only the final states with $m=0$ and odd l are excited and the $\mathcal{Y}^*(\theta)$ takes the form

$$\mathcal{Y}^*(\theta) = -B_{10} e^{i\pi \mu_1} \sqrt{\frac{3}{4\pi}} \cos \theta, \quad (28)$$

where B_{10} represents only a simple multiplicative factor.

IV. CONSTANT SCALED ENERGY SPECTRA

In order to test the semiclassical theory outlined in Sec. III we have evaluated Eq. (24) to obtain semiclassical approximations for both diamagnetic and Stark photoabsorption spectra of nonhydrogenic atoms. The semiclassical approach only requires information about the classical orbits of the corresponding hydrogenic system and so, in this section, we give the Hamiltonians for both of these systems. We show how the Hamiltonians can be scaled to remove their separate dependence on electron energy and field strength and how to modify the closed-orbit expressions to account for the scaling.

A. Hamiltonians and scaled variables

The dynamics of a highly excited hydrogen atom (in a state with $m=0$) in a static external field aligned along the z axis is described by a single-particle, nonrelativistic Hamiltonian which, in atomic units and cylindrical coordinates (ρ, ϕ, z) , is

$$H = \frac{1}{2} (p_\rho^2 + p_z^2) - \frac{1}{(\rho^2 + z^2)^{1/2}} + H_{\text{ext}}, \quad (29)$$

where $H_{\text{ext}} = \frac{1}{8}\gamma^2\rho^2$ ($H_{\text{ext}} = zF$) is the Hamiltonian of the external magnetic (electric) field of strength γ (F) measured in atomic units.

The classical motion of Hamiltonian (29) exhibits an important scaling property. If we transform variables according to

$$\tilde{\mathbf{r}} = w\mathbf{r}, \quad \tilde{\mathbf{p}} = w^{-1/2}\mathbf{p}, \quad \tilde{t} = w^{3/2}t, \quad (30)$$

where the scaling parameter $w = \gamma^{2/3}$ ($w = F^{1/2}$) for the magnetic (electric) field, then the classical motion is governed by the *scaled* Hamiltonian

$$\tilde{H} = \frac{1}{2}(\tilde{p}_\rho^2 + \tilde{p}_z^2) - \frac{1}{(\tilde{\rho}^2 + \tilde{z}^2)^{1/2}} + \tilde{H}_{\text{ext}} = \varepsilon, \quad (31)$$

which is simply the original Hamiltonian of Eq. (29) multiplied by w^{-1} . The (scaled) Hamiltonian of the external magnetic (electric) field, $\tilde{H}_{\text{ext}} = \frac{1}{8}\tilde{\rho}^2$ ($\tilde{H}_{\text{ext}} = \tilde{z}$), does not depend on the strength of the field. Consequently, all properties of the classical system no longer depend on the energy E and field strength separately but only on a single parameter, the *scaled energy*, which for the magnetic (electric) field problem is given by $\varepsilon = E\gamma^{-2/3}$ ($\varepsilon = EF^{-1/2}$).

In order to solve numerically the equations of motion generated by Hamiltonian (31) it is convenient to make a regularizing transformation that removes the Coulomb singularity. For the case considered here, where $m=0$, this can be achieved by transforming to semi-parabolic coordinates, (u, v) , where

$$u^2 = \tilde{r} + \tilde{z}, \quad v^2 = \tilde{r} - \tilde{z}, \quad \text{with } \tilde{r} = (\tilde{\rho}^2 + \tilde{z}^2)^{1/2} \quad (32)$$

and with conjugate momenta, $p_u = du/d\tau$, $p_v = dv/d\tau$, defined with respect to a rescaled time, τ , given by

$$\frac{d\tau}{dt} = \frac{1}{2\tilde{r}(t)} = \frac{1}{(u^2 + v^2)}. \quad (33)$$

On transforming to semiparabolic coordinates our final Hamiltonian becomes

$$\mathcal{H} = \frac{1}{2}(p_u^2 + p_v^2) - \varepsilon(u^2 + v^2) + \mathcal{H}_{\text{ext}} - 2 \equiv 0, \quad (34)$$

where for the diamagnetic (Stark) problem $\mathcal{H}_{\text{ext}} = \frac{1}{8}u^2v^2(u^2 + v^2)$ [$\mathcal{H}_{\text{ext}} = \frac{1}{2}(u^4 - v^4)$].

The scaling transformation, Eq. (30), has an important consequence for the quantum system. Solving the Schrödinger equation corresponding to Hamiltonian (31) at fixed scaled energy leads to a set of eigenvalues $\{w_i\}$ corresponding to a set of energies $\{E_i = \varepsilon w_i\}$. Thus, the field strength is not entirely eliminated from the quantum problem: each E_i corresponds to a different value of an effective Planck's constant which, for the magnetic (electric) field problem, is $\hbar_{\text{eff}} = \gamma^{1/3}$ ($\hbar_{\text{eff}} = F^{1/4}$). However, all of the eigenvalues now correspond to a *single* classical regime and the semiclassical limit, $\hbar_{\text{eff}} \rightarrow 0$, can be studied by decreasing the field strength while keeping ε constant.

It should be noted that, in contrast to the diamagnetic problem, the Stark Hamiltonian (34) is separable and the motion is therefore integrable. Thus, we can quantize this

system using Einstein-Brillouin-Keller (EBK) quantization rules; for states well below the Stark barrier ($\varepsilon \ll -2.0$), these are

$$\frac{1}{2\pi} \oint p_u du = \left(n_u + \frac{1}{2}\right) F^{-1/4}, \quad n_u = 0, 1, \dots \quad (35)$$

$$\frac{1}{2\pi} \oint p_v dv = \left(n_v + \frac{1}{2}\right) F^{-1/4}, \quad n_v = 0, 1, \dots \quad (36)$$

The connection between EBK quantization of the electric field problem and closed-orbit theory has been investigated by Gao and Delos [30].

B. Closed-orbit formula for fixed scaled energy spectra

Certain modifications have to be made to the closed-orbit formula given in Sec. III before it can be used to obtain constant scaled energy spectra. Here, we follow Main *et al.* [31] and consider a reduced absorption rate which is defined as

$$R(\hbar_{\text{eff}}, \varepsilon) = \frac{f(\hbar_{\text{eff}}, \varepsilon)}{\hbar_{\text{eff}}^{1/2}(E - E_i)}, \quad (37)$$

where $\hbar_{\text{eff}} = \gamma^{1/3}$ ($\hbar_{\text{eff}} = F^{1/4}$) and $\varepsilon = E\gamma^{-2/3}$ ($\varepsilon = EF^{-1/2}$) is the scaled energy for the magnetic (electric) field case. As in Sec. III, the oscillatory part of $f(\hbar_{\text{eff}}, \varepsilon)$ can be expressed in terms of the coefficients \mathcal{N}_j ; see Eq. (27). The advantage of the reduced absorption rate is that the amplitude of the contributions of the (not core-scattered) closed orbits is independent of \hbar_{eff} .

On substituting the scaled variables, Eq. (30), into Eq. (20) for the \mathcal{N}_j 's we obtain the following expression:

$$\mathcal{N}_j = \left\{ \mathcal{D}_j(\theta_i^j) + \sum_{k,p} \mathcal{N}_k \mathcal{B}_j^{k,p}(\theta_i^j) \right\} \sum_n \hbar_{\text{eff}}^{\nu_j/2} \mathcal{A}_j^n e^{i\Delta_j^n}, \quad (38)$$

where $\nu_j = 2$ for $\theta_i^j = 0$ or $\theta_i^j = \pi$ and $\nu_j = 1$ otherwise. The phase of the semiclassical wave function has been written as

$$\Delta_j^n = \frac{2\pi}{\hbar_{\text{eff}}} \tilde{S}_j^n - \frac{\alpha_j^n \pi}{2} - \phi_j, \quad (39)$$

where the *scaled* action for an orbit, j , is defined as

$$\tilde{S}_j = \frac{1}{2\pi} \oint_{\tilde{\mathbf{j}}} \tilde{\mathbf{p}} \cdot d\tilde{\mathbf{q}} = \frac{\hbar_{\text{eff}}}{2\pi} S_j. \quad (40)$$

The factor of $\hbar_{\text{eff}}^{\nu_j/2}$ in Eq. (38) arises from the effect of the scaling transformation on the semiclassical amplitude, \mathcal{A}_j^n , which, for $\theta_i^j \neq 0, \pi$, can now be written as [27]

$$\mathcal{A}_j^n = |\sin \theta_f^j \sin \theta_i^j|^{1/2} |2^{1/2} \cos \frac{\theta_i^j}{2} \cos \frac{\theta_f^j}{2} m_{12}|^{-1/2}, \quad (41)$$

and, for $\theta_i^j = 0$ or $\theta_i^j = \pi$, as

$$\mathcal{A}_j^n = |2^{1/2} m_{12}|^{-1}, \quad (42)$$

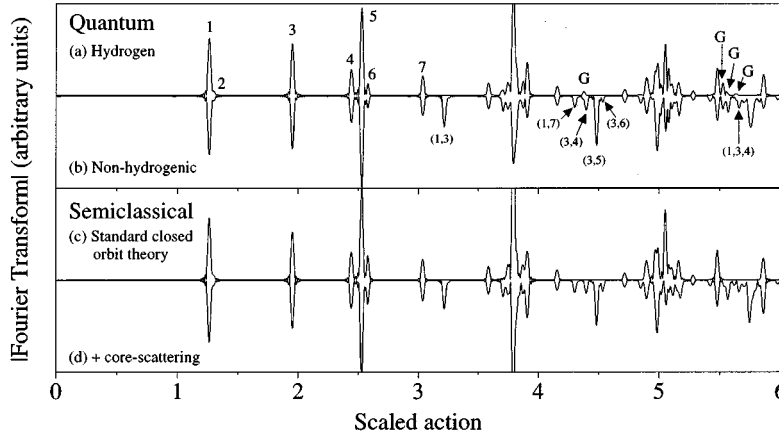


FIG. 1. Fourier transforms of the photoexcitation spectra (from the ground state) of Rydberg atoms in a magnetic field at constant scaled energy $\varepsilon = -0.3$ ($m=0$, odd parity states, $\gamma^{-1/3}$ in the range 60–120). (a) Quantum result for hydrogen. The peaks appear at the actions of the closed orbits (see Table I for list). Also visible are ghost peaks (marked G). (b) Quantum results for a nonhydrogenic atom with $\mu_1=0.5$; core-scattered peaks appear at the sum of actions of periodic orbits. (c) Standard semiclassical calculation for the hydrogen atom, in good agreement with (a), but not with (b). (d) Our semiclassical calculation, which goes beyond the standard closed-orbit theory by including core-scattering effects and successfully reproduces the quantum nonhydrogenic spectrum.

where m_{12} is an element of the 2×2 stability matrix for the n th return to the nucleus of the j th closed orbit, evaluated using semiparabolic coordinates, Eq. (32) [29].

V. ITERATIVE SOLUTION

In order to obtain a semiclassical approximation to the scaled energy photoabsorption spectrum, we need to solve Eq. (38) for the \mathcal{N}_j 's; for convenience, we rewrite Eq. (38) in the form

$$\mathcal{N}_j = \left\{ \mathcal{D}_j + \sum_k \mathcal{N}_k \mathcal{B}_k^j \right\} \hbar_{\text{eff}}^{\nu_j/2} \mathcal{A}_j^n e^{i\Delta_j^n}, \quad (43)$$

where an implicit summation over repetitions n of all closed orbits j has been assumed. In order to proceed, we set the \mathcal{N}_k 's on the left-hand side of Eq. (43) to zero and obtain a zeroth-order approximation to the solution, namely,

$$\mathcal{N}_{k_0}^{(0)} = \hbar_{\text{eff}}^{\nu_0/2} \mathcal{D}_{k_0} \mathcal{A}_{k_0}^{n_0} e^{i\Delta_{k_0}^{n_0}}, \quad (44)$$

where again an implicit summation over repetitions of the orbits, which we have indexed by k_0 , is assumed. For the first return to the nucleus, $n_0=1$, Eq. (44) is precisely the standard closed-orbit result obtained by Gao and Delos [24]. To obtain the next approximation we substitute this expression for $\mathcal{N}_k^{(0)}$ into the right-hand side of Eq. (43) giving

$$\mathcal{N}_{k_0}^{(1)} = \mathcal{N}_{k_0}^{(0)} + \hbar_{\text{eff}}^{(\nu_1 + \nu_0)/2} \sum_{k_1} \mathcal{D}_{k_1} \mathcal{A}_{k_1}^{n_1} \mathcal{A}_{k_0}^{n_0} \mathcal{B}_{k_0}^{k_1} e^{i(\Delta_{k_1}^{n_1} + \Delta_{k_0}^{n_0})}, \quad (45)$$

where now we have an implicit summation over repetitions n_1 as well as n_0 . We see that the expression for $\mathcal{N}_{k_0}^{(1)}$ brings in combinations of two hydrogenic actions, $\Delta_{k_1}^{n_1} + \Delta_{k_0}^{n_0}$. Continuing in this way, we arrive the p th order of the approximation:

$$\begin{aligned} \mathcal{N}_{k_0}^{(p)} = & \mathcal{N}_{k_0}^{(p-1)} + \hbar_{\text{eff}}^{(\nu_p + \dots + \nu_0)/2} \sum_{k_p} \dots \sum_{k_0} \mathcal{D}_{k_p} \\ & \times \mathcal{A}_{k_p}^{n_p} \dots \mathcal{A}_{k_0}^{n_0} \mathcal{B}_{k_{p-1}}^{k_p} \dots \mathcal{B}_{k_0}^{k_1} e^{i(\Delta_{k_p}^{n_p} + \dots + \Delta_{k_0}^{n_0})}. \quad (46) \end{aligned}$$

Thus the p th correction term combines $p+1$ primitive actions resulting from p encounters with the core. The correction due to the p th iteration is $O(\hbar_{\text{eff}}^{\nu_p/2})$. Hence, for small \hbar_{eff} , convergence is assured with successive iterations. Equation (46) shows that the modulations of the photoabsorption probability induced by the core scattering are at least a factor of $\sqrt{\hbar_{\text{eff}}}$ smaller than the modulations induced by the hydrogenic closed orbits. Hence, far in the semiclassical limit, the contribution of an individual core-scattered closed orbit should vanish. However, when going to longer and longer actions, the core-scattered orbits proliferate exponentially and may give contributions to the photoabsorption cross section.

The same approach can be used at values of ε where the hydrogenic classical motion is regular. In this case, the core scattering is seen to be the same mechanism as the ‘‘torus-hopping’’ observed in model potential calculations [15,22].

VI. RESULTS

A. Diamagnetic recurrence spectra

We have used our semiclassical method, which combines closed-orbit theory with core scattering to calculate recurrence spectra for diamagnetic nonhydrogenic Rydberg atoms. In Figs. 1(a)–1(d) we compare the results for $m=0$, odd- l , and $\gamma^{-1/3}=60$ –120 in a magnetic field with constant scaled energy $\varepsilon = -0.3$. The photoabsorption spectrum is calculated from an initial s state using π polarization. Both the ‘‘quantum’’ (using the numerical method described in Ref. [12]) and the ‘‘semiclassical’’ (using the method described in the previous sections) spectra are computed and further Fourier transformed with respect to $\gamma^{-1/3}$ to obtain

TABLE I. Correspondence between the integers labeling the peaks in Fig. 1 and the periodic orbits described following the nomenclature of [3].

1	2	3	4	5	6	7
V_1^1	V_1	R_2^1	V_2^1	V_2^2	V_2	R_3^1

recurrence spectra. Note that, contrary to Ref. [31], we plot the modulus of the Fourier transform, not the modulus squared.

Figure 1(a) shows the Fourier transformed (recurrence) spectrum of hydrogen. Figure 1(b) shows the quantum spectrum for an atom with $\mu_1=0.5$ (comparable to Cs, which has $\mu_1=0.57$ and $\mu_{l \geq 3}$ negligible.). Figure 1(c) shows the standard closed-orbit result with $\mu_1=0.5$ while Fig. 1(d) shows the current version with the same quantum defect. One can see that, even for quite small values of \hbar_{eff} ($n \approx 77-154$), there is a substantial difference between hydrogen and the core-scattered case. Each peak in the Fourier transform is associated with a closed orbit. It appears at the scaled action \tilde{S}_j of the orbit with an amplitude proportional to A_j . The core-scattered contributions (or “combination recurrences”) are the peaks located at the sums $\tilde{S}_j + \tilde{S}_k$. Further we can see that the standard closed-orbit result reproduces only the hydrogen results, while the current version with core scattering gives excellent agreement with the fully quantal nonhydrogenic case.

The integers in Fig. 1(a) indicate primary orbits. Table I gives the correspondence between these integers and the periodic orbits, following the convention of Ref. [3]. The pairs of integers in Fig. 1(b) indicate combinations of orbits: the core-scattered peaks. A few peaks present in Fig. 1(a) (indicated with a G) are not found even in the new semiclassical results. They correspond to ghost peaks [23], in other words, orbits that appear in the quantum spectrum below the energy of the bifurcation at which they are born. The triple integers indicate a peak due to double scattering: an action corresponding to a combination of three orbits.

The Fourier transforms converged after two iterations, that is Eq. (46) was solved up to $p=2$, indicating that scattering beyond double scattering is unimportant. In Fig. 2 we have compared our results for one iteration in Fig. 2(a) (i.e., the hydrogenic case), two iterations in Fig. 2(b) (single scattering), and three and four iterations in Figs. 2(c) and 2(d) corresponding to double and triple scattering. It may be seen that most new features are accounted for by single scattering except for the small peak, indicated with an arrow in Fig. 2(c), which corresponds to a combination of three periodic orbits. No significant differences are discerned between Fig. 2(c) and Fig. 2(d) indicating that for this range of $\hbar_{\text{eff}} = \gamma^{1/3}$ the results are converged for powers equal to or higher than \hbar_{eff}^2 .

The major disagreement between the semiclassical and quantum results is in the peak for the third harmonic of V_1^1 . However, there is already a comparatively similar discrepancy for this peak between Figs. 1(a) and 1(c), the hydrogenic case. Such discrepancies occur when the semiclassical amplitude is near a singularity, for example, when a winding number is nearly rational. In that case the semiclassical result overestimates the quantum amplitude—the dis-

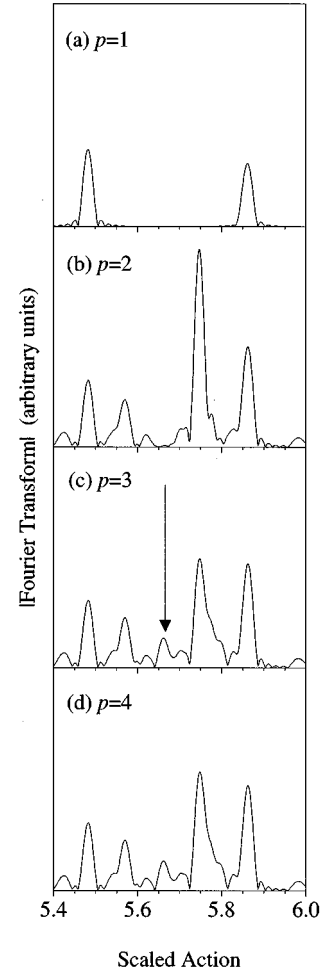


FIG. 2. Fourier transforms of the photoexcitation spectrum (from the ground state) for a nonhydrogenic atom with $\mu_1=0.5$ in a magnetic field at constant scaled energy $\varepsilon = -0.3$ ($m=0$, odd-parity states, $\gamma^{-1/3}$ in the range 60–120) calculated with our closed-orbit plus core-scattering approach. The figures show the evolution of the spectrum with increasing number of iterations. (a) One iteration (hydrogenic—no core scattering); (b) two iterations giving rise to core-scattered peaks; (c) three iterations giving a double core-scattered peak (indicated by the arrow); (d) four iterations—little different from (c) showing that the sum has converged.

crepancy increases for larger \hbar_{eff} . Nevertheless the semiclassical results agree with the quantum in predicting a reduction of about 30% in amplitude of this peak due to the back-scattered shadow of the core. Very strong reductions in amplitudes of higher harmonics were seen in [11], which looked at very low-lying levels ($n \approx 10-30$) where comparison with semiclassical results is more difficult.

B. Stark recurrence spectra

We have also used our semiclassical method to calculate recurrence spectra for nonhydrogenic atoms in static electric fields. In Figs. 3(a)–3(d) we compare results for lithium at $\varepsilon = -3.0$ with $m=0$ and $F^{-1/4} = 150-230$ using photoexcitation from an initial s state and π polarization. Figure 3(a) shows the quantum spectrum for hydrogen. The spectrum is dominated by the two straight-line orbits parallel to the electric field—one that runs towards the anode, the other towards

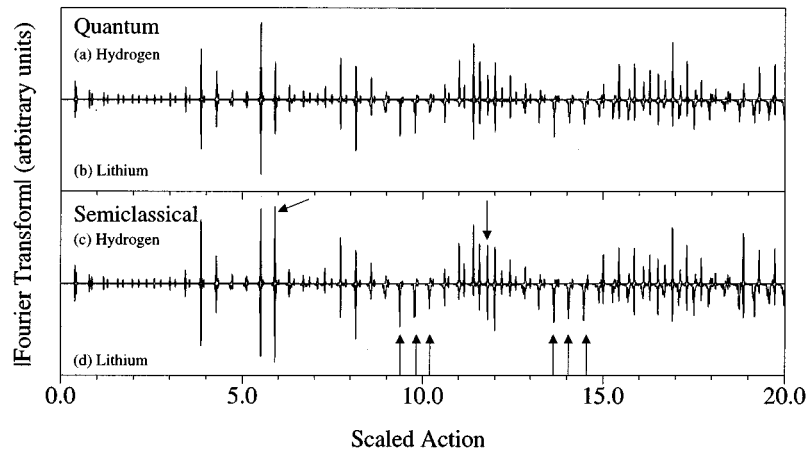


FIG. 3. Fourier transforms of the photoexcitation spectra (from the ground state) of Rydberg atoms in a static electric field at constant scaled energy $\varepsilon = -3.0$ ($m=0$ with $F^{-1/4}$ in the range 150–230). (a) Quantum result for hydrogen. The spectrum is dominated by the two straight-line orbits parallel to the electric field—one which runs towards the anode, the other towards the cathode—and their harmonics. (b) Quantum result for lithium ($\mu_0=0.4$, $\mu_{l \geq 1}=0$). For this system, and at this resolution, the core-scattered peaks are less easily identified. The major difference between the lithium and hydrogenic spectra is in the heights of the peaks. At higher scaled actions, some slight shift in the positions of the peaks can also be discerned. (c) Standard semiclassical calculation for the hydrogen atom, in good agreement with (a), but not with (b). The main discrepancies in the heights of the peaks, for example, at $\tilde{S}=5.0$ and its harmonic at $\tilde{S}=11.8$, which are indicated with arrows, are due to classical resonances. (d) Our semiclassical calculation for lithium. The positions of some of the core-scattered peaks close to $\tilde{S}=10$ and $\tilde{S}=14$ are indicated by arrows. The overall agreement with (b) is very good.

the cathode—and their harmonics. Figure 3(b) shows the quantum spectrum for lithium ($\mu_0=0.4$, while the other quantum defects are much smaller). For this system, and at this resolution, the core-scattered peaks are less easily identified. The major difference between the lithium [Fig. 3(b)] and hydrogenic spectra [Fig. 3(a)] is in the heights of the peaks. At higher scaled actions, some slight shift in the positions of the peaks can also be discerned. Figure 3(c) shows the results of using the standard closed-orbit formula with $\mu_0=0.4$ while Fig. 3(d) shows those obtained with the semiclassical version. In this case, four iterations were required to produce converged results. As with the diamagnetic case, we see that the standard closed-orbit result reproduces only the hydrogenic spectrum while the current version with core scattering is in excellent agreement with the fully quantal lithium spectrum; a few of the core-scattered peaks near $\tilde{S}=10$ and 14 have been indicated by arrows in Fig. 3(d). The main disagreements between Fig. 3(d) and Fig. 3(b) lie

in the heights of some of the peaks, for example, at $\tilde{S}=5.9$ and its harmonic at $\tilde{S}=11.8$ (indicated by arrows), with those obtained from the semiclassical calculation being larger than those of the quantum. Again, these are due to resonances in the semiclassical amplitude and can also be seen by comparing the quantum and semiclassical hydrogenic spectra [Figs. 3(a) and 3(c)]. These resonances reduce agreement between the quantum and semiclassical calculations for lithium as amplitudes that are too large are appearing in the core scattering process and leading to overestimates of the amplitudes of the core-scattered peaks. However, for higher levels, these discrepancies become less pronounced as the quantum approaches the semiclassical limit. We have found that where the hydrogenic amplitudes are well described the corresponding core-scattered peaks are in excellent agreement with the quantum results.

In Fig. 4 we compare the Fourier transforms of the Stark

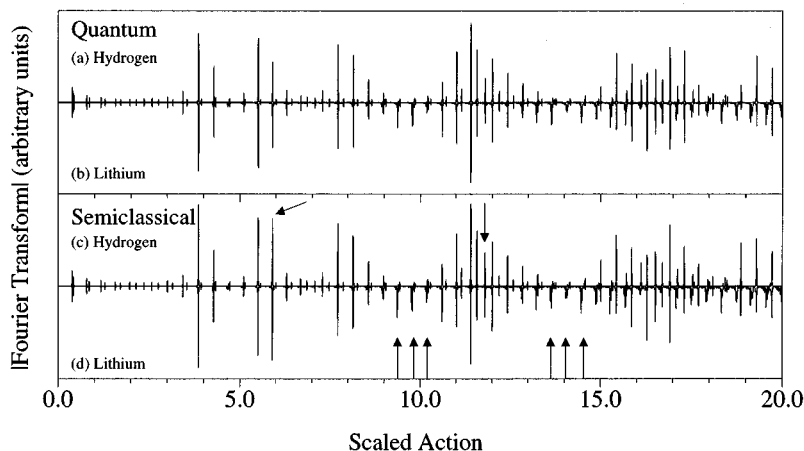


FIG. 4. As for Fig. 3 but with $F^{-1/4}$ in the range 300–460. For these very high levels, agreement between quantum and semiclassical calculations is very good. Discrepancies between the quantum and semiclassical results due to classical resonances are less pronounced than in Fig. 3.

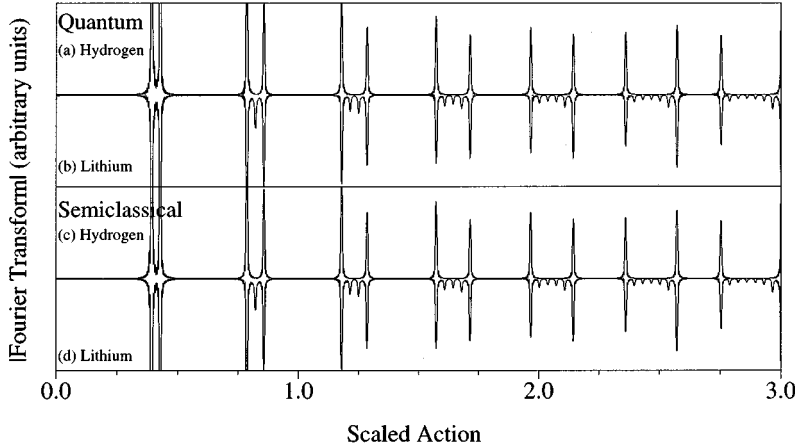


FIG. 5. Magnification of the Stark spectra as for Fig. 3 but for $\tilde{S} \leq 3$ and $F^{-1/4}$ in the range 40–240, showing the small core-scattered peaks, visible at this high resolution, which lie between peaks corresponding to repetitions of the two parallel orbits. The additional peaks visible in the lithium spectrum are produced by a core-scattering process between the two parallel orbits. Again, the core-scattered peaks are well reproduced by our semiclassical calculation.

spectrum of lithium and hydrogen at $\varepsilon = -3.0$, $m = 0$, as in Fig. 3, but this time for the range $F^{-1/4} = 300\text{--}460$. For these high levels, agreement between the quantum and semiclassical spectra is very good for both hydrogen and lithium. In particular, we see that the discrepancies in the heights of the peaks between the hydrogenic quantum and semiclassical calculations [Figs. 4(a) and 4(c), respectively] are less pronounced than in Fig. 3. For example, the large peaks at actions $\tilde{S} = 5.9$ and its harmonic at $\tilde{S} = 11.8$ (again indicated by arrows) are in much closer agreement for the 300–460 range. As a result of this better agreement, there is improved agreement between the quantum and semiclassical spectra of lithium (Figs. 4(b) and 4(d), respectively), especially at higher scaled actions. The comparison between Figs. 3 and 4 also shows that the amplitudes of the core-scattered peaks decrease with a higher power of \hbar_{eff} than the amplitudes of the normal (unscattered) peaks, in agreement with the theoretical prediction, Eq. (46). For example, the three core-scattered peaks around action $\tilde{S} = 10$, which exist only in the lithium spectra (they are indicated by arrows) and the three core-scattered peaks around action $\tilde{S} = 14$ are relatively smaller in Fig. 4 than in Fig. 3.

As mentioned above, the core-scattered peaks are less easily identified in the Stark spectrum of lithium. However, in Fig. 5 we show a magnification of the recurrence spectrum in the range $F^{-1/4} = 40\text{--}240$ for $\tilde{S} \leq 3$. At this magnification it is possible to see the small core-scattered peaks that lie between the peaks corresponding to repetitions of the two parallel orbits. These additional peaks visible in the lithium spectrum, Fig. 5(b), are produced by the core-scattering process between the two parallel orbits. Again, these core-scattered peaks are well reproduced by our semiclassical calculation, Fig. 5(d).

VII. DISCUSSION AND CONCLUSIONS

We have demonstrated that core-scattered modulations for atomic diamagnetic as well as Stark spectra obtained from accurate fully quantal calculations are reproduced with a model employing only a few hydrogenic periodic orbits in an expansion including higher-order terms in Planck’s constant. The agreement between this computationally very simple model and the large accurate quantal calculations is in fact excellent, with significant disagreement only at actions cor-

responding to orbits in the vicinity of bifurcations, including ghosts; in this work we have not employed the normal form approach to correct the semiclassical amplitude in the vicinity of the bifurcations. However, we have found that if the hydrogenic amplitudes are reduced by the appropriate amount near a divergence, any remaining discrepancy in the core-scattered peaks is removed. In any case, for small values of \hbar_{eff} , the discrepancy is small.

Hence we find that the seemingly “chaotic” behavior of core-scattering systems may be quantitatively accounted for by a simple analytical expression in terms of a contribution from a few periodic orbits (which are stable at low scaled energy) and the appropriate quantum defects. This makes the approach a simple and computationally inexpensive procedure for analyzing experimental atomic spectra. A fully semiclassical procedure [27] requires about 2500 orbits to analyze diamagnetic spectra (which must be recalculated for each atom), in comparison with the procedure presented here, which requires only about 30 hydrogenic orbits.

Nevertheless the extent to which the dynamics of the Rydberg atoms in fields is accounted for by the fully chaotic model-potential dynamics, rather than being an instance of diffractive scattering, and hence a breakdown of standard periodic orbit theory, is an interesting one. In the future we will present a detailed comparison between the two methods.

However, we have already found that agreement with model potential results is more qualitative, deteriorating rapidly for small quantum defects. Further we find that for the case of a helium model potential a deflection through an angle of 180 degrees (and hence scattering between the orbit parallel and that antiparallel to the electric field) is not possible. Hence these contributions are absent in model-potential Stark spectra but are present in quantum Stark spectra. The recurrence spectrum for the helium atom in an electric field—similar to the one plotted in Fig. 5—will display core-scattered peaks for the “exact” spectrum, but not for a model-potential calculation. We will also wish to consider the density of states, rather than simply the photoabsorption spectra. In that case, the procedure of employing Liapunov exponents calculated by “switching off” the core potential at the start and final return of each orbit to the core region would not seem justifiable.

The de Broglie wavelength of the electron approaching the core is of the order of one atomic unit, of the same order

as the ionic core. Hence we conclude that to ensure quantitative results the inclusion of diffractive effects is essential.

ACKNOWLEDGMENTS

This work has been supported in part by EPSRC and also by the British Council through the Alliance Programme.

Laboratoire Kastler-Brossel is unité associée 18 au CNRS, and unité de recherche de l'École Normale Supérieure et de l'Université Pierre et Marie Curie, associée au CNRS. CPU time on a Cray C98 has been provided by IDRIS. Two of us (T.S.M. and P.A.D.) thank the Department of Mathematics, Royal Holloway, University of London, for their support and hospitality during the initial preparation of this work.

-
- [1] M.C. Gutzwiller, *Chaos in Classical and Quantum Mechanics* (Springer-Verlag, New York, 1990).
- [2] *Irregular Atomic Systems and Quantum Chaos*, edited by J.-C. Gay (Gordon and Breach, London, 1992).
- [3] A. Holle, J. Main, G. Wiebusch, H. Rottke, and K.H. Welge, *Phys. Rev. Lett.* **61**, 161 (1988).
- [4] H. Hasegawa, M. Robnik, and G. Wunner, *Prog. Theor. Phys. Suppl.* **98**, 198 (1989).
- [5] H. Friedrich and D. Wintgen, *Phys. Rep.* **183**, 37 (1989).
- [6] D. Wintgen, *Phys. Rev. Lett.* **58**, 1589 (1987).
- [7] M.L. Du and J.B. Delos, *Phys. Rev. A* **38**, 1896 (1988); **38**, 1913 (1988).
- [8] E.B. Bogomolny, *Zh. Éksp. Teor. Fiz.* **96**, 487 (1989) [*Sov. Phys. JETP* **69**, 275 (1989)].
- [9] G. Alber, *Z. Phys. D* **14**, 307 (1989).
- [10] U. Eichmann, K. Richter, D. Wintgen, and W. Sandner, *Phys. Rev. Lett.* **61**, 2438 (1988).
- [11] T.S. Monteiro and G. Wunner, *Phys. Rev. Lett.* **65**, 1100 (1990).
- [12] D. Delande, K.T. Taylor, M.H. Halley, T. van der Veldt, W. Vassen, and W. Hogervorst, *J. Phys. B* **27**, 2771 (1994).
- [13] G. Raithel, H. Held, L. Marmet, and H. Walther, *J. Phys. B* **27**, 2849 (1994).
- [14] M. Courtney, H. Jiao, N. Spellmeyer, and D. Kleppner, *Phys. Rev. Lett.* **73**, 1340 (1994).
- [15] M. Courtney, N. Spellmeyer, H. Jiao, and D. Kleppner, *Phys. Rev. A* **51**, 3604 (1995).
- [16] P.F. O'Mahony and K.T. Taylor, *Phys. Rev. Lett.* **57**, 2931 (1986).
- [17] P.F. O'Mahony, *Phys. Rev. Lett.* **63**, 2653 (1989).
- [18] M.H. Halley, D. Delande, and K.T. Taylor, *J. Phys. B* **26**, 1775 (1993).
- [19] C.W. Clark and K.T. Taylor, *J. Phys. B* **15**, 1175 (1982).
- [20] M.J. Seaton, *Rep. Prog. Phys.* **46**, 167 (1983).
- [21] W. Jans, T.S. Monteiro, W. Schweizer, and P.A. Dando, *J. Phys. A* **26**, 3187 (1993).
- [22] P.A. Dando, T.S. Monteiro, W. Jans, and W. Schweizer, *Prog. Theor. Phys. Suppl.* **116**, 403 (1994).
- [23] M. Kuš, F. Haake, and D. Delande, *Phys. Rev. Lett.* **71**, 2167 (1993).
- [24] J. Gao, J.B. Delos, and M. Baruch, *Phys. Rev. A* **46**, 1449 (1992); J. Gao and J.B. Delos, *ibid.* **46**, 1455 (1992).
- [25] We should note at this point that Gao and Delos [24] were studying photoabsorption spectra of nonhydrogenic atoms in static electric fields for $E > 0$. In this case, there exists only one classical orbit of the corresponding hydrogenic system that is closed at the nucleus and hence neglecting core scattering between orbits can be justified.
- [26] P.A. Dando, T.S. Monteiro, D. Delande, and K.T. Taylor, *Phys. Rev. Lett.* **74**, 1099 (1995).
- [27] B. Hüpper, J. Main, and G. Wunner, *Phys. Rev. Lett.* **74**, 2650 (1995); B. Hüpper, J. Main, and G. Wunner, *Phys. Rev. A* **53**, 744 (1996).
- [28] V.P. Maslov and M.V. Fedoriuk, *Semiclassical Approximation in Quantum Mechanics* (Reidel, Boston, 1981).
- [29] J.-M. Mao, J. Shaw, and J.B. Delos, *J. Stat. Phys.* **68**, 51 (1992).
- [30] J. Gao and J.B. Delos, *Phys. Rev. A* **49**, 869 (1994).
- [31] J. Main, G. Wiebusch, K. Welge, J. Shaw, and J.B. Delos, *Phys. Rev. A* **49**, 847 (1994).